

Rectifying the thermal Brownian motion of three-dimensional asymmetric objects

Peer-reviewed author version

VAN DEN BROEK, Martijn & VAN DEN BROECK, Christian (2008) Rectifying the thermal Brownian motion of three-dimensional asymmetric objects. In: PHYSICAL REVIEW E, 78(1).

DOI: [10.1103/PhysRevE%2E78%2E011102](https://doi.org/10.1103/PhysRevE.78.011102)

Handle: <http://hdl.handle.net/1942/8433>

Rectifying the thermal Brownian motion of three-dimensional asymmetric objects

M. van den Broek and C. Van den Broeck
Hasselt University, B-3590 Diepenbeek, Belgium

We extend the analysis of a thermal Brownian motor reported in Phys. Rev. Lett. **93**, 090601 (2004) by C. Van den Broeck, R. Kawai, and P. Meurs to a three-dimensional configuration. We calculate the friction coefficient, diffusion coefficient, and drift velocity as a function of shape and present estimates based on physically realistic parameter values.

PACS numbers: 05.70.Ln, 05.40.Jc, 51.10.+y, 51.20.+d

I. INTRODUCTION

Spectacular advances in bio- and nanotechnology make it possible, not only to measure or observe, but also to manipulate and construct objects at a very small scale. At the same time there is growing interest in techniques which can add functionality. In particular, the development of molecular engines is a theme which has received great attention over the last two decades. The appearance of fluctuations in small systems has led to new concepts for characterizing or operating such devices, exploiting rather than fighting these very same fluctuations.

These so-called Brownian motors [1, 2] have an additional theoretical interest through their relation with the old issue of Maxwell demons and the second law of thermodynamics. In return, this theoretical connection allows to make statements on the efficiency of such engines [3] or to transform them from engines into mini-refrigerators [4, 5]. Most of the studies on Brownian motors start with an ad hoc separation of systematic and noise terms, based on linear Langevin equations. This approach however offers little insight into the origin of the rectification of random fluctuations. As pointed out by van Kampen [6], the rectification of nonlinear fluctuations cannot be addressed starting from the standard Langevin description with additive Gaussian white noise. In [7, 8] a theoretical and numerical study of a thermal engine is presented in which rectification arises at the level of nonlinear response. The analysis therein starts from a microscopic description based on Newton's laws of motion. There is another related distinct feature of the model: the asymmetry of the thermal engine lies in the geometry of the motor itself, in contrast to the asymmetry imposed by the application of an external potential, appearing in the so-called flashing and rocking ratchet models.

The characteristic properties of the engine, such as the friction coefficient, the speed and the diffusion coefficient, are calculated exactly in [7, 8] and are found to be in excellent agreement with the results from hard disk molecular dynamics. However, the results are reported in dimensionless units, in part due to the fact that the analysis was, for reasons of simplicity and for comparison with molecular dynamics, limited to the case of two dimensions. In view of the technological interest of motors in bio- and nanotechnology, we report here a full and

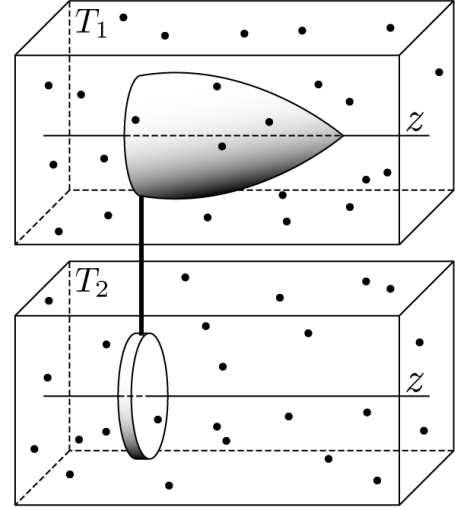


FIG. 1: The two-reservoir model of the thermal engine: two solid objects are confined in separate containers (scaled down for illustration purposes) that contain gases at temperatures T_1 and T_2 . The objects are assembled with a rigid connection. The ensemble can move freely along the z -axis.

detailed analysis of the three-dimensional version.

This paper is organized as follows. First, the model, notations, and working hypothesis are introduced in section II. The calculation method, based on the kinetic theory of gases, is presented in section III, with a discussion of the analytical solution following in section IV. Finally, in section V we report and discuss the results for the friction coefficient, diffusion coefficient, and drift velocity as a function of shape and present estimates based on physically realistic parameter values.

II. THE MODEL

The model presented in [7] reproduces in a simplified way the principle ingredients of Feynman's ratchet and pawl mechanism [9]: a temperature difference between two reservoirs and the presence in at least one reservoir of an asymmetric object. The construction, extended to the case of three spatial dimensions, is as follows. We consider any number of reservoirs (denoted by index i), each containing a gas at equilibrium at a temperature T_i .

Fig. 1 gives a schematic picture of the two-reservoir system. Solid objects with no internal degrees of freedom, called ‘motor units’, are located inside the containers. These objects are coupled rigidly to each other, so that the motor moves as a single entity, with total mass M , along a given straight axis, corresponding to its single translational degree of freedom. For simplicity, we disregard any rotational degree of freedom (for a detailed discussion of this case, see [5]).

Due to collisions with the gas particles (mass m), the motor will change its velocity $V(t)$ in the course of time t . The statistics of these collisions can be described under the assumption of molecular chaos, which is valid when the gases are in the high Knudsen number regime and the containers are large enough to avoid acoustic and other boundary effects. In addition, the shape of the units’ surfaces must be such that no re-collisions with the motor occur, namely for convex and closed shapes. With these assumptions, the precollisional velocities are random and uncorrelated. Hence the time evolution of the probability $P(V, t)$ that the motor has speed V at time t can be described by a master equation:

$$\frac{\partial P(V, t)}{\partial t} = \int dV' [W(V|V')P(V', t) - W(V'|V)P(V, t)]. \quad (1)$$

Here $W(V|V')$ represents the transition probability per unit time for the motor to change its speed from V' to V .

III. KINETIC THEORY

In this section we study the collisions of gas particles from either temperature reservoir with a motor part and derive the resulting total transition probability $W(V|V')$ for the motor to change speed from V' to V . We introduce a Cartesian coordinate system (x, y, z) where the z -axis points along the free direction of movement of the motor.

A. Conservation rules

A gas particle will, upon collision with a motor unit, undergo an instantaneous change of velocity from $\vec{v}' = (v'_x, v'_y, v'_z)$ before collision to $\vec{v} = (v_x, v_y, v_z)$ afterwards. Due to conservation of momentum along the free z -direction, one has:

$$mv'_z + MV' = mv_z + MV. \quad (2)$$

In addition, when the collision is perfectly elastic, the total energy is conserved:

$$\begin{aligned} \frac{1}{2}MV'^2 + \frac{1}{2}mv'^2_x + \frac{1}{2}mv'^2_y + \frac{1}{2}mv'^2_z \\ = \frac{1}{2}MV^2 + \frac{1}{2}mv^2_x + \frac{1}{2}mv^2_y + \frac{1}{2}mv^2_z. \end{aligned} \quad (3)$$

We will also suppose that the collision is described in terms of a (short-range) central force, implying that the component of the momentum of the gas particle along any direction tangential to the surface of the motor is conserved. The orientation of the tangent plane to the

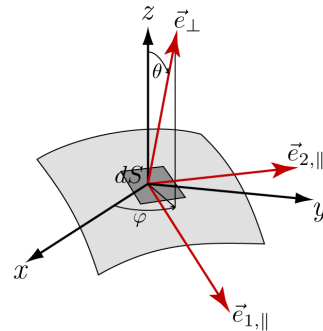


FIG. 2: (Color online) The orientation of an infinitesimal surface element dS is represented by an outer-pointing unit normal vector \vec{e}_\perp and determined by the spherical coordinates φ and θ . The polar angle θ is measured from the z -axis, which is chosen as the free direction of movement of the motor. x, y complete the Cartesian coordinate system and the azimuthal angle φ starts from the x -axis. Two orthogonal unit vectors $\vec{e}_{1,\parallel}$ and $\vec{e}_{2,\parallel}$ determine the plane that is tangent to the motor unit in dS .

motor surface is determined uniquely by a normal outward vector on an infinitesimal element dS of the surface at the point of collision. In spherical coordinates, this normal vector is given by

$$\vec{e}_\perp|_{\text{cart}} \doteq (\sin \theta \cos \varphi, \sin \theta \sin \varphi, \cos \theta), \quad (4)$$

with θ the polar angle from the z -axis ($0 \leq \theta \leq \pi$) and φ the azimuthal angle in the xy -plane from the x -axis ($0 \leq \varphi < 2\pi$), cf. Fig. 2. We also introduce two mutually perpendicular unit vectors within the tangent plane:

$$\vec{e}_{1,\parallel} \doteq (\cos \theta \cos \varphi, \cos \theta \sin \varphi, -\sin \theta), \quad (5)$$

$$\vec{e}_{2,\parallel} \doteq (-\sin \varphi, \cos \varphi, 0), \quad (6)$$

so that we can write the conservation of tangential momentum as

$$\vec{v}' \cdot \vec{e}_{1,\parallel} = \vec{v} \cdot \vec{e}_{1,\parallel}, \quad (7)$$

$$\vec{v}' \cdot \vec{e}_{2,\parallel} = \vec{v} \cdot \vec{e}_{2,\parallel}. \quad (8)$$

Solving the conservation rules [Eqs. (2,3,7,8)] for V, v_x, v_y, v_z leads to the following expression for the post-collisional speed V of the motor in terms of the precollisional speeds:

$$\begin{aligned} V = V' \\ + \frac{2 \frac{m}{M} \cos^2 \theta}{1 + \frac{m}{M} \cos^2 \theta} (v'_x \tan \theta \cos \varphi + v'_y \tan \theta \sin \varphi + v'_z - V'). \end{aligned} \quad (9)$$

$$(10)$$

B. Transition probability

The motor is subject to random collisions by gas particles from the different reservoirs i . The particle density and velocity distribution in reservoir i are denoted by ρ_i and $\phi_i(v_x, v_y, v_z)$, respectively. The contribution $dW_i(V|V')$ to the total transition probability $W(V|V')$, coming from collisions on an infinitesimal surface element dS_i of the motor unit in reservoir i , can then be found by considering the number of gas particles that collide with this surface element dS_i in a unit time step:

$$\begin{aligned} dW_i(V|V') &= dS_i \int_{-\infty}^{+\infty} dv'_x \int_{-\infty}^{+\infty} dv'_y \int_{-\infty}^{+\infty} dv'_z \\ &\times H[(\vec{V}' - \vec{v}') \cdot \vec{e}_\perp] |(\vec{V}' - \vec{v}') \cdot \vec{e}_\perp| \rho_i \phi_i(v'_x, v'_y, v'_z) \\ &\times \delta[V - V'] \\ &- B(\theta)(\tan \theta \cos \varphi v'_x + \tan \theta \sin \varphi v'_y + v'_z - V'). \end{aligned} \quad (11)$$

Here H represents the Heaviside function, δ the Dirac distribution, and

$$B(\theta) = \frac{2 \frac{m}{M} \cos^2 \theta}{1 + \frac{m}{M} \cos^2 \theta}. \quad (12)$$

The Dirac delta distribution selects those particles that produce the required postcollisional speed V , following the collision rules [Eq. (10)]. Assuming that the velocity distribution of the gas particles is Maxwellian at the reservoir temperature T_i ,

$$\phi_i(v_x, v_y, v_z) = \left(\frac{m}{2\pi k_B T_i} \right)^{3/2} \exp \left[-\frac{m(v_x^2 + v_y^2 + v_z^2)}{2k_B T_i} \right], \quad (13)$$

the integrals over v'_x, v'_y, v'_z in Eq. (11) can be calculated explicitly. The total transition probability for the motor to change velocity from V' to V in a unit time, is then found by integrating $dW_i(V|V')$ over the surface S_i of each motor part and summing over all the reservoirs i :

$$\begin{aligned} W(V|V') &= \frac{1}{4} \sum_i \rho_i \sqrt{\frac{m}{2\pi k_B T_i}} \\ &\times \left((V - V') H[V - V'] \int_{S_i, \cos \theta > 0} dS_i \right. \\ &+ (V' - V) H[V' - V] \left. \int_{S_i, \cos \theta < 0} dS_i \right) \left(\frac{M}{m \cos \theta} + \cos \theta \right)^2 \\ &\times \exp \left[-\frac{m}{2k_B T_i} \cos^2 \theta \left(V' + \frac{1}{2} \left(1 + \frac{M}{m \cos^2 \theta} \right) (V - V') \right)^2 \right]. \end{aligned} \quad (14)$$

We note that in the case of a single reservoir or for multiple reservoirs at the same temperature, the transition probability satisfies the following relation:

$$W(V|V') P^{eq}(V') = W(-V'| - V) P^{eq}(-V), \quad (15)$$

with $P^{eq}(V)$ the Maxwell Boltzmann distribution for the speed V of the motor unit (at the temperature of the reservoir(s)). This is in agreement with the general principle of detailed balance in a system at equilibrium [10].

IV. SOLUTION METHOD

We follow the method of [8] to solve the master equation [Eq. (1)] for the moments of the motor velocity,

$$\langle V^n \rangle = \int_{-\infty}^{\infty} P(V, t) V^n dV. \quad (16)$$

This method is based on the van Kampen $1/\Omega$ expansion [6].

A. Solution of the master equation

It is convenient to scale the motor velocity V to a dimensionless variable

$$X = \sqrt{\frac{M}{k_B T_{\text{eff}}}} V, \quad (17)$$

with the effective temperature T_{eff} to be determined self-consistently from the condition $\langle X^2 \rangle = 1$ in steady state operation. We can expand the integrand in Eq. (1) in a Taylor series about X' :

$$\frac{\partial P(X, t)}{\partial t} = \sum_{n=1}^{\infty} \frac{(-1)^n}{n!} \frac{d^n}{dX^n} \{J_n(X) P(X, t)\}. \quad (18)$$

Here the ‘jump moments’ are given by

$$J_n(X) = \int \Delta X^n W(X; \Delta X) d\Delta X, \quad (19)$$

with $W(X'; \Delta X) = W(X|X')$ and $\Delta X = X' - X$. Using Eq. (18) a coupled set of equations for the time evolution of the moments $\langle X^n \rangle$ can then be constructed:

$$\frac{\partial \langle X^n \rangle}{\partial t} = \sum_{k=1}^n \binom{n}{k} \langle X^{n-k} J_k(X) \rangle, \quad (20)$$

with $\binom{n}{k}$ the binomial coefficients.

The exact expression for the jump moments $J_n(X)$ is obtained by integration over ΔX in Eq. (19). In terms of parabolic cylinder functions [11],

$$\begin{aligned} D_n(z) &= (\exp[-z^2/4]/\Gamma[-n]) \\ &\times \int_0^\infty \exp[-zx - x^2/2] x^{-n-1} dx \quad (\text{for } n < 0), \end{aligned} \quad (21)$$

and the Gamma function (Γ), the result reads:

$$J_n(X) = \frac{2^n}{\sqrt{2\pi}} \Gamma[n+2] \left(\sqrt{\frac{M}{m}} \right)^n \quad (22)$$

$$\times \sum_i \rho_i \sqrt{\frac{k_B T_i}{m}} \left(\sqrt{\frac{T_i}{T_{\text{eff}}}} \right)^n \quad (23)$$

$$\times \int_{S_i} dS_i \left(\cos \theta + \frac{M}{m} \frac{1}{\cos \theta} \right)^{-n} \quad (24)$$

$$\times \exp \left[-\frac{1}{4} \frac{m}{M} \frac{T_{\text{eff}}}{T_i} X^2 \cos^2 \theta \right] \quad (25)$$

$$\times D_{-n-2} \left[\frac{1}{2} \sqrt{\frac{m}{M}} \sqrt{\frac{T_{\text{eff}}}{T_i}} X \cos \theta \right]. \quad (26)$$

An exact solution of Eq. (20) is not available. We therefore turn to a perturbational approach in terms of the parameter

$$\varepsilon = \sqrt{m/M}. \quad (27)$$

This is consistent with the observation that the mass M of the motor is expected to be much larger than the mass m of the gas particles. Even for a motor with dimensions of nanometers operating in a gaseous environment, ε is of order of 10^{-3} .

The expansion of the parabolic cylinder functions is given by

$$\begin{aligned} 2^{-n/2} \Gamma[n+2] D_{-n-2}(z) &= \Gamma\left[\frac{n+2}{2}\right] - \sqrt{2} \Gamma\left[\frac{n+3}{2}\right] z \\ &+ \frac{2n+3}{4} \Gamma\left[\frac{n+2}{3}\right] z^2 - \frac{2n+3}{6\sqrt{2}} \Gamma\left[\frac{n+3}{2}\right] z^3 \\ &+ \frac{4n^2+12n+11}{96} \Gamma[(2+n)/2] z^4 + O(z^5). \end{aligned} \quad (28)$$

Introducing a scaled time $\tau = \varepsilon^2 t$, we find the following expansion for the equation of the first moment:

$$\begin{aligned} \frac{\partial \langle X \rangle}{\partial \tau} &= \sum_i \rho_i \sqrt{\frac{k_B T_i}{m}} \left[\varepsilon^{-1} \sqrt{\frac{T_i}{T_{\text{eff}}}} \sigma_{1,i} - 2 \sqrt{\frac{2}{\pi}} \langle X \rangle \sigma_{2,i} \right. \\ &+ \varepsilon \left(\sqrt{\frac{T_{\text{eff}}}{T_i}} \langle X^2 \rangle - \sqrt{\frac{T_i}{T_{\text{eff}}}} \right) \sigma_{3,i} \\ &+ \frac{\varepsilon^2}{3} \sqrt{\frac{2}{\pi}} \left(6 \langle X \rangle - \frac{T_{\text{eff}}}{T_i} \langle X^3 \rangle \right) \sigma_{4,i} \\ &\left. + \varepsilon^3 \left(\sqrt{\frac{T_i}{T_{\text{eff}}}} - \sqrt{\frac{T_{\text{eff}}}{T_i}} \langle X^2 \rangle \right) \sigma_{5,i} \right] + O(\varepsilon^4). \end{aligned} \quad (29)$$

The geometry of the motor is contained in the shape factors $\sigma_{n,i}$, defined as:

$$\sigma_{n,i} = \int_{S_i} dS_i \cos^n \theta. \quad (30)$$

At this point we remark that the azimuthal angle φ has dropped out, and that the geometric dependency is determined only by the (polar) angle θ between the surface and the direction of movement. Also note that the term in ε^{-1} in Eq. (29) is zero by application of Gauss' theorem:

$$\sigma_{1,i} = \int_{S_i} dS_i \cos \theta = \int_{S_i} dS_i \vec{e}_\perp \cdot \vec{e}_z = \int_{V_i} dV_i (\nabla \cdot \vec{e}_z) = 0, \quad (31)$$

where the latter integral is over the interior volume V_i of a motor part. This is consistent with the fact that there is no net macroscopic force acting on the motor. The net motion that will be revealed below is the effect of fluctuations only.

Similarly, for the equation of the second moment, one finds the following expansion:

$$\begin{aligned} \frac{\partial \langle X^2 \rangle}{\partial \tau} &= \sum_i \rho_i \sqrt{\frac{k_B T_i}{m}} \left[-4 \sqrt{\frac{2}{\pi}} \left(-\frac{T_i}{T_{\text{eff}}} + \langle X^2 \rangle \right) \sigma_i^2 \right. \\ &- 2\varepsilon \left(4 \sqrt{\frac{T_i}{T_{\text{eff}}}} \langle X \rangle - \sqrt{\frac{T_{\text{eff}}}{T_i}} \langle X^3 \rangle \right) \sigma_i^3 \\ &\left. + 2\varepsilon^2 \sqrt{\frac{2}{\pi}} \left(-4 \frac{T_i}{T_{\text{eff}}} + 5 \langle X^2 \rangle - \frac{1}{3} \frac{T_{\text{eff}}}{T_i} \langle X^4 \rangle \right) \sigma_i^4 \right] + O(\varepsilon^3). \end{aligned} \quad (32)$$

B. Linear relaxation

To order ε^0 , Eq. (29) reduces to a linear relaxation law $M \partial_t \langle V \rangle = -\gamma \langle V \rangle$ with $\gamma = \sum_i \gamma_i$ the sum of linear friction coefficients γ_i of each part of the object:

$$\gamma_i = 4 \rho_i \sqrt{\frac{k_B T_i m}{2\pi}} \sigma_{2,i} = \rho_i \bar{v}_i \sigma_{2,i}, \quad (33)$$

where $\rho_i = m \rho_i$ is the mass density of the gas, $\bar{v}_i = \sqrt{8k_B T_i / (\pi m)}$ is the mean gas velocity, and $\sigma_{2,i}$ is a geometric factor.

C. Nonlinearity: Steady state directed motion

If a constant temperature difference between the reservoirs can be maintained for a time longer than the relaxation time M/γ , the probability distribution will relax to its steady state value. Restricting ourselves to the first two moments, we turn to the steady state solution of Eqs. (29) and (32). First, from Eq. (32) we determine the effective temperature T_{eff} , which was defined earlier by the condition $\langle X^2 \rangle = 1$. To lowest order, ε^0 , we find that T_{eff} is the weighted average of the reservoir temperatures:

$$T_{\text{eff}} = \frac{\sum_i \gamma_i T_i}{\sum_i \gamma_i} = \frac{\sum_i \rho_i \sigma_{2,i} T_i^{3/2}}{\sum_i \rho_i \sigma_{2,i} T_i^{1/2}}. \quad (34)$$

TABLE I: The geometric moments σ_2 and σ_3 for some basic three-dimensional shapes. The lowest orders σ_2 and σ_3 ($\sigma_1 = 0$) are tabulated in terms of the total surface area S of the geometry. For illustrations of the shapes and their parameters, see Fig. 3.

Shape	σ_2/S	σ_3/S	Surface S
Disk	1	0	$2\pi r^2$
Blade	1	0	$2lw$
Sphere	$1/3$	0	$4\pi r^2$
Cone	$\sin \alpha$	$\sin \alpha(\sin \alpha - 1)$	$\pi r^2(1 + \csc \alpha)$
Pyramid	$\sin \alpha$	$\sin \alpha(\sin \alpha - 1)$	$\frac{1}{4}nr^2 \cot \frac{\pi}{n} (1 + \csc \alpha)$
Spherical cap	$\frac{\cos 2\alpha + 5 \cos \alpha + 6}{3 \cos \alpha + 9}$	$\frac{\sin^4 \alpha}{\cos 2\alpha + 4 \cos \alpha - 5}$	$\pi r^2(3 + \cos \alpha)/(1 + \cos \alpha)$
Spherical cone	$\frac{3 \sin^2 \alpha - 2 \cos^3 \alpha + 2}{3 \sin \alpha - 6 \cos \alpha + 6}$	$\frac{2 \sin^4 \alpha + \cos^4 \alpha - 1}{4 \cos \alpha - 2 \sin \alpha - 4}$	$\pi r^2 \csc \alpha(1 + 2 \tan(\alpha/2))$

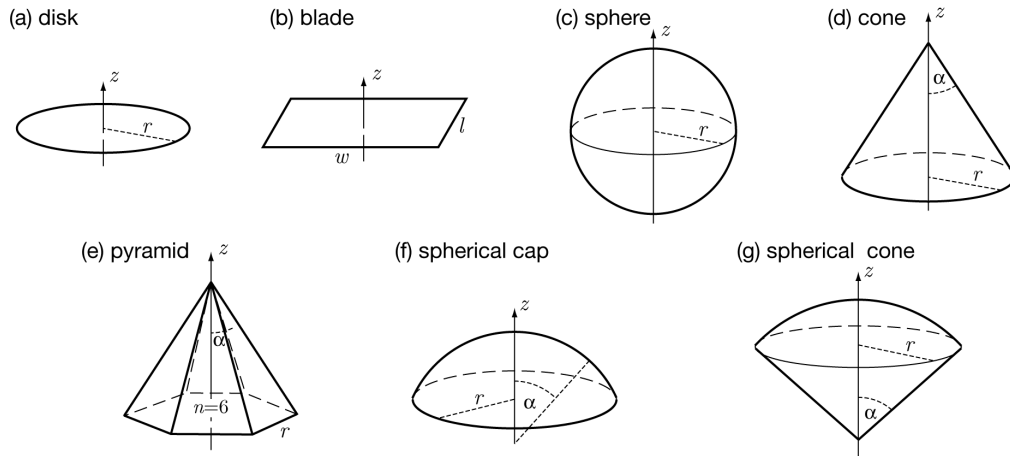


FIG. 3: Examples of simple three-dimensional geometries that can be treated analytically. The parameters that determine the relative areas of the surfaces are indicated in the illustrations.

Solving Eq. (29) to order ε^0 leads to a zero average drift speed $\langle X \rangle = 0$. Rectification of the thermal fluctuations occurs at higher levels of the expansion and it is necessary to include nonlinear terms. Solving Eq. (29) up to order ε gives us an expression to lowest order for the average drift speed of the motor:

$$\begin{aligned}
 \langle V \rangle &= \sqrt{\frac{m}{M}} \sqrt{\frac{\pi k_B T_{\text{eff}}}{8M}} \frac{\sum_i \rho_i \left(\frac{T_i}{T_{\text{eff}}} - 1 \right) \sigma_{3,i}}{\sum_i \rho_i \sqrt{\frac{T_i}{T_{\text{eff}}}} \sigma_{2,i}} \\
 &= \sqrt{\frac{m}{M}} \sqrt{\frac{\pi k_B}{8M}} \frac{\sum_i \sum_j \rho_i \rho_j \sigma_{3,i} \sigma_{2,j} (T_i - T_j) \sqrt{T_j}}{(\sum_i \rho_i \sqrt{T_i} \sigma_{2,i})^2}.
 \end{aligned} \tag{35}$$

V. RESULTS AND DISCUSSION

A. Friction and diffusion coefficients

Although not directly related to the main topic of this work, we briefly pause to discuss the new result for the linear friction coefficient, given in Eq. (33). Together with results from Table I for the geometric factors σ_2 this result provides the explicit expression for the linear

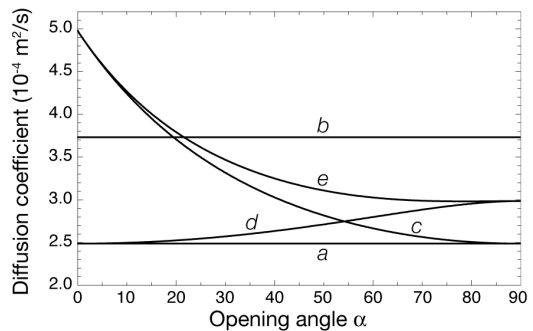


FIG. 4: Diffusion coefficients of objects with different geometry but identical cross section πr^2 ($r = 100$ nm) in highly diluted argon gas (10^{19} m^{-3} particles, mean free path $2.3 \mu\text{m}$) at 299 K temperature. The geometries are (a) a disk, (b) a sphere, (c) a cone, (d) a spherical cap, and (e) a spherical cone. See Fig. 3 for illustrations. For (c,d,e) the shapes and hence the diffusion coefficients depend on an opening angle α .

friction coefficient of corresponding basic shapes. The result for a spherical shape with radius r ,

$$\gamma = \frac{4}{3} \pi r^2 \rho_i \bar{v}_i, \tag{36}$$

is in agreement with the result found in [12]. In combination with the Einstein relation $D = k_B T / \gamma$, we also obtain the explicit formulas for the corresponding diffusion coefficients D . As an illustration, numerical values are given in Fig. 4 for various shapes of cross section πr^2 , $r = 100$ nm. To be concrete, we consider highly diluted argon gas (density 10^{19} m^{-3}) leading to diffusion coefficients of the order of $3 \times 10^{-4} \text{ m}^2/\text{s}$, and corresponding friction coefficients of order $1.5 \times 10^{-17} \text{ Ns/m}$. As expected, the conical shapes have higher diffusion coefficients and lower friction as one considers smaller opening angles α .

B. Equilibrium

When the reservoirs are all at the same temperature, $T_i = T$, we find $T_{\text{eff}} = T$, and the distribution of the moments is Gaussian:

$$\langle X \rangle = 0, \langle X^2 \rangle = 1, \langle X^3 \rangle = 0, \langle X^4 \rangle = 3, \dots \quad (37)$$

The notion that it is impossible to achieve directed motion (or equivalently, to extract work) from a system in thermal equilibrium is confirmed. At least two reservoirs at different temperature are necessary to break detailed balance and make possible the rectification of thermal fluctuations.

C. Asymmetry

The geometry of the motor units enters into the expression of the average speed via de shape factors σ_2 and σ_3 . In table I, we have reproduced these quantities for the objects depicted in Fig. 3. As is clear from symmetry arguments, the appearance of systematic motion in one direction requires, apart from non-equilibrium conditions, also the breaking of the spatial symmetry in the system. One easily verifies from Eq. (30) that

$$\sigma_{n,i} = 0, \quad n \text{ odd}, \quad (38)$$

when the surface of a motor element possesses reflection symmetry along the z -axis, the direction of motion. Consistent with this symmetry observation we find that the drift speed of the motor in steady state is indeed zero at lowest order in the perturbation when $\sigma_{3,i} = 0$, cf. Eq. (35). It is however interesting to note that reflection symmetry is a sufficient but not a necessary condition for $\sigma_{3,i} = 0$, and hence for obtaining zero sustained motion (at least in this order of the approximation). Consider for example a spherical cone, see Fig. 5. For a specific opening angle of $\approx 55^\circ$ $\sigma_{3,i}$ becomes zero, even though there is no reflection symmetry. A similar discussion can be applied to higher orders corrections in the ε -expansion (featuring the appearance of the higher shape factors σ_5 , σ_7 , and so on) indicating that there are special shapes which will have a very low average speed even though there are no immediate symmetry reasons to expect so.

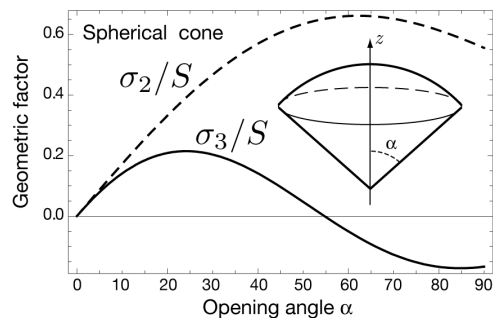


FIG. 5: The geometric factors σ_2/S and σ_3/S as a function of the opening angle α for a spherical cone, with S the surface area. While σ_2 appears in the expression for the friction coefficient, σ_3 relates to the drift speed of the motor. When the geometry of the surface exhibits symmetry along the z -axis (the direction of movement), σ_3 is zero, and the motor shows no directed motion. The spherical cone is an example of a class of shapes for which σ_3 can become zero, and hence the drift speed (at least to the first approximation), without however showing reflection symmetry. For this particular case, $\sigma_3 = 0$ for $\alpha \approx 55^\circ$.

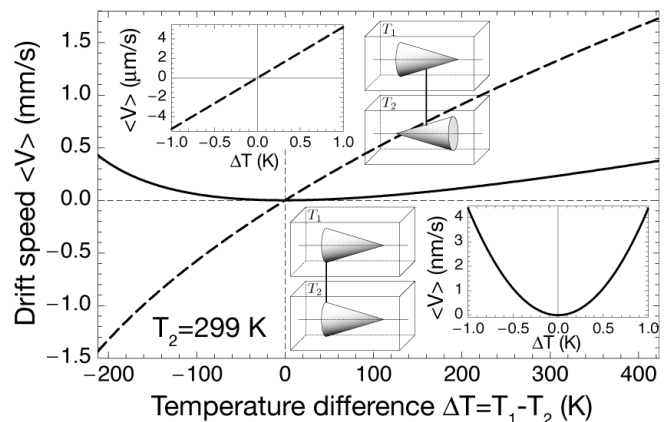


FIG. 6: The drift speed as a function of the temperature difference $\Delta T = T_1 - T_2$ between the reservoirs for two configurations with identical motor units: parallel (solid curves and lower inset) and antiparallel (dashed curves and upper inset). The units are cone-shaped (opening angle 30°) and the motor mass is 1000 kDa. Both reservoirs are filled with argon gas of same density and T_2 is fixed at 299 K. For small ΔT (see insets), the dependence is parabolic for the parallel setup and linear for the antiparallel setup. The drift speed is of order nm/s (parallel) and $\mu\text{m/s}$ (antiparallel) for $\Delta T \approx 1$ K.

D. Temperature gradient

For simplicity we limit the discussion of the drift velocity, in particular in relation to the applied temperature gradient, to the case of two reservoirs. Furthermore, the impact of the geometry is most clearly demonstrated when the motor units have an identical shape in both reservoirs. There are then two possibilities, namely either the units have the same orientation (parallel), or they are

pointing in opposite direction (antiparallel), see Fig. 6 for a schematic representation. For the first scenario, with $\sigma_{2,1} = \sigma_{2,2} = \sigma_2$ and $\sigma_{3,1} = \sigma_{3,2} = \sigma_3$, Eq. (35) yields:

$$\langle V \rangle_e = \sqrt{\frac{m}{M}} \sqrt{\frac{\pi k_B}{8M}} \frac{\rho_1 \rho_2 (T_1 - T_2) (\sqrt{T_2} - \sqrt{T_1})}{(\rho_1 \sqrt{T_1} + \rho_2 \sqrt{T_2})^2} \frac{\sigma_3}{\sigma_2}. \quad (39)$$

For the second scenario, careful consideration of the sign of $\cos \theta$ in Eq. (30) leads us to write $\sigma_{2,1} = \sigma_{2,2} = \sigma_2$ as in the first scenario, but now when $\sigma_{3,1} = \sigma_3$, it follows that $\sigma_{3,2} = -\sigma_3$. The expression for the drift speed thus becomes:

$$\langle V \rangle_o = \sqrt{\frac{m}{M}} \sqrt{\frac{\pi k_B}{8M}} \frac{\rho_1 \rho_2 (T_1 - T_2) (\sqrt{T_1} + \sqrt{T_2})}{(\rho_1 \sqrt{T_1} + \rho_2 \sqrt{T_2})^2} \frac{\sigma_3}{\sigma_2}. \quad (40)$$

One striking feature of these results is that the drift velocity is scale-invariant. This is a general property: both σ_2 and σ_3 scale linearly with the total surface S of the motor units. As they appear in the denominator and the nominator respectively in Eqs. (39, 40), the scale dependence cancels out. This becomes even more apparent for the particular cases presented in Table I, where σ_2/S and σ_3/S are expressed in topological terms. Note that the scale invariance of the drift speed is only valid with respect to the scale of the entire motor. The relative proportions of separate motor units do matter. Note also that scale invariance applies when disregarding the dependence on the mass M . For comparison with a physically realistic situation, we assume a constant density of the motor, so that the drift velocity will decrease with increasing size of an object, through its $1/M$ -dependence.

To investigate the departure from the equilibrium state, we consider small deviations of T_1 and T_2 about the average T ,

$$T_1 = T + \frac{\Delta T}{2}, \quad T_2 = T - \frac{\Delta T}{2}, \quad (41)$$

so that for $\Delta T/T \ll 1$ the drift speeds tend to:

$$\langle V \rangle_e \rightarrow -\frac{1}{16} \sqrt{\frac{\pi}{2}} \sqrt{\frac{m}{M}} \frac{\rho_1 \rho_2}{(\rho_1 + \rho_2)^2} \frac{\sigma_3}{\sigma_2} \sqrt{\frac{k_B T}{M}} \left(\frac{\Delta T}{T} \right)^2, \quad (42)$$

$$\langle V \rangle_o \rightarrow \frac{1}{4} \sqrt{\frac{\pi}{2}} \sqrt{\frac{m}{M}} \frac{\rho_1 \rho_2}{(\rho_1 + \rho_2)^2} \frac{\sigma_3}{\sigma_2} \sqrt{\frac{k_B T}{M}} \left(\frac{\Delta T}{T} \right). \quad (43)$$

We note that the respective orientation of the motor elements, parallel or antiparallel, plays a crucial role. In the first case the sustained average displacement is always in the same direction (that of $-\sigma_3$), indifferent of the sign of ΔT . This was to be expected because there is an additional symmetry in the system: the interchange of the temperature reservoirs has no effect. From the point of view of irreversible thermodynamics, this situation is special since there is no linear relation between the thermodynamic force (the temperature gradient) and flux (the resulting speed of the motor). For the second

TABLE II: Values for the drift speed of the motor, as predicted by theory. Realizations of the motor at different length scales from micrometers to nanometers are presented. The motor units are modeled as silica (SiO_2) cone-shaped objects, located in two reservoirs containing argon gas at temperatures 299.0 K and 299.1 K. For constant motor mass, the speed increases as the opening angle α of the cone decreases.

Motor mass (kDa)	$\alpha = 30^\circ$	$\alpha = 5^\circ$	$\alpha = 30^\circ$	$\alpha = 5^\circ$
	Cylinder base (nm)		Drift speed ($\mu\text{m/s}$)	
10^{10}	2600	1400	5.2×10^{-8}	9.5×10^{-8}
10^7	260	140	5.2×10^{-5}	9.5×10^{-5}
10^6	120	55	5.2×10^{-4}	9.5×10^{-4}
10^5	63	29	5.2×10^{-3}	9.5×10^{-3}
10^4	26	14	0.052	0.095
1000	12	6.3	0.52	0.95
100	5.5	2.9	5.2	9.5
10	2.6	1.4	52	95

case of antiparallel alignment, one observes the usual situation of linear response between thermodynamic force and flux [2, 3]: equilibrium is a point of flux reversal, the direction of net motion reversing with ΔT -inversion.

As an illustration, we reproduce, in table II, explicit values for the drift speed in the case of a single asymmetric unit, namely a cylindrically symmetric cone, positioned in antiparallel alignment in the two reservoirs under physically realistic conditions. The degree of asymmetry is described by a single parameter, the opening angle α . The geometric factors σ_2 and σ_3 are known analytically (see Table I) and we find the following simple expression for the drift speed:

$$\langle V \rangle = \sqrt{\frac{m}{M}} \sqrt{\frac{\pi k_B}{8M}} \frac{\rho_1 \rho_2 (T_1 - T_2) (\sqrt{T_1} + \sqrt{T_2})}{(\rho_1 \sqrt{T_1} + \rho_2 \sqrt{T_2})^2} (\sin \alpha - 1). \quad (44)$$

The drift speed will become zero for $\alpha = 90^\circ$, namely when the cone loses its asymmetry and reduces to a flat disk. A natural question is whether there is an optimal opening angle α_o that maximizes the drift speed. For a fixed cross section, one finds $\alpha_o = \sec^{-1}[\sqrt{(1 + \sqrt{5})/2}] \approx 38^\circ$. If, on the other hand, one assumes that the mass is kept constant, a maximal speed is reached for an infinitely sharp cone.

Note finally the very strong size-dependence: objects of 20 nm cover their length 5 times per second, for 5 nm size objects this becomes 1200 times per second.

VI. CONCLUSION

We have calculated, on the basis of an exact microscopic theory, the properties of a thermal Brownian motor in a three-dimensional setup. When detailed balance is broken by the application of a temperature gradient, a

systematic net speed appears, as given in Eq. (35). As an example, for a motor consisting of cone-shaped silica units of size 20 nm, one obtains a drift speed of about 0.1 $\mu\text{m/s}$ when subject to 0.1 K temperature difference in a gaseous environment. It remains to be seen whether the

predictions of our theoretical analysis (involving various simplifications such as molecular chaos, elastic and normal interactions between gas particles and motor, expansion in mass ratio) provide a realistic estimate, especially for motors operating in a viscous environment.

-
- [1] F. Jülicher, A. Ajdari, and J. Prost, *Rev. Mod. Phys.* **69**, 1269 (1997).
 - [2] P. Reimann, *Phys. Rep.* **361**, 57 (2002).
 - [3] C. Van den Broeck, *Phys. Rev. Lett.* **95**, 190602 (2005); C. Van den Broeck, *Adv. Chem. Phys.* **135**, 189 (2007).
 - [4] C. Van den Broeck and R. Kawai, *Phys. Rev. Lett.* **96**, 210601 (2006) .
 - [5] M. van den Broek and C. Van den Broeck, to appear.
 - [6] N.G. van Kampen, *Stochastic Processes in Physics and Chemistry* (North-Holland, Amsterdam, 1981).
 - [7] C. Van den Broeck, R. Kawai, and P. Meurs, *Phys. Rev. Lett.* **93**, 090601 (2004).
 - [8] P. Meurs, C. Van den Broeck, and A. Garcia, *Phys. Rev. E* **70**, 051109 (2004); C. Van den Broeck, P. Meurs, and R. Kawai, *New J. Phys.* **7**, 10 (2005); P. Meurs and C. Van den Broeck, *J. Phys.: Condens. Matter* **17**, S3673 (2005).
 - [9] R.P. Feynman, R.B. Leighton, and M. Sands, *The Feynman Lectures on Physics I* (Addison-Wesley, Reading, MA, 1963).
 - [10] L. Onsager, *Phys. Rev.* **37**, 405 (1931); *ibid.* **38**, 2265 (1931).
 - [11] I. S. Gradshteyn and I. M. Ryzhik, *Table of Integrals, Series, and Products* (Academic, New York, 1980).
 - [12] P. S. Epstein, *Phys. Rev.* **23**, 710 (1924).